Journal of Material Cycles and Waste Management (2024) 26:2741–2753
https://doi.org/10.1007/s10163-024-01999-3

ORIGINAL ARTICLE

Assessing the impact of recycled mortar powder on the strength, durability and microstructural characteristics of geopolymer concrete

Paramveer Singh[1] · **Kanish Kapoor**[1]

Received: 19 September 2023 / Accepted: 3 June 2024 / Published online: 14 June 2024

Abstract

The recycling of concrete waste and its utilization in new concrete production can be a great contribution to a sustainable environment. In the present study, the impact of recycled mortar powder (RMP) was accessed on fly ash (FA) based geopolymer concrete (GC). The RMP was substituted with FA in the range of 0–50%. The durability properties such as capillary suction test (CST), initial surface absorption test (ISAT) and acid attack test were accessed and strength property was also evaluated in terms of compressive strength at ambient curing. Further, the ultrasonic pulse velocity (UPV) test and electrical resistivity test were also conducted for all GC mixes. The present study outcome shows that the overall properties of GC improved with the addition of RMP up to 30%. Moreover, the addition of RMP provides the early activation of GC due to calcium (Ca) compounds present in RMP. The microstructural characteristics of GC mixes were analyzed using field emission scanning electronic microscopy (FESEM) along with Fourier transform infrared (FTIR) spectroscopy and it revealed that the presence of Ca compound in RMP form additional nucleation sites i.e., calcium/sodium alumina-silicate hydrate gel with a polymeric chain which enhance the overall properties of the GC.

Keywords Fly ash · Recycled mortar powder · Durability properties · Capillary suction test · Acid attack test · Microstructural analysis

Introduction

Geopolymer concrete (GC) is a no cement concrete which will become a new generation of concrete in the construction world. The GC can be a viable substitute for conventional cement concrete in the coming years. The Portland Cement (PC) binder of conventional cement concrete is produced from natural resources such as limestone and clay which emits huge amounts of CO_2 during their production [1]. In contrast, the binder used in GC is manufactured from by-products that are high in alumina and silicate, such as fly ash (FA), metakaolin (MK) and ground granulated blast furnace slag (GGBS) [2]. To reduce CO_2 emissions and achieve sustainability, the binder used in the manufacturing of GC may be an effective substitute for PC [3]. The GC is generally made up of binders rich in alumina and silicate along with alkaline solutions and aggregates. The FA are widely utilized as the principal binder in GC because they are inexpensive and widely available [4]. The FA is produced through the combustion of coals in thermal plants and generated in massive amounts which consume the landfills [5]. Globally, 71 million tons to 1 billion tons of FA is generated through thermal plants [6]. A huge amount of FA is generally disposed of in landfills which in turn increases air and land pollution [7]. Therefore, the consumption of FA in GC reduces the burden on landfills which aids in reducing land pollution. In the geopolymer process, sodium hydroxide (SH) along with sodium silicate (SS) are primarily utilized as an alkaline solution. In geopolymerization, the alkaline solutions (SH and SS) dissolve the silica (Si) and alumina (Al) of the binder through polymerization to produce the polymeric chain as a final product [8]. Numerous studies are going on the production of GC using different combinations of binders and alkaline solutions. One of the key concerns in the production of the GC is the slow geopolymeric reaction and low strength at the initial stage of ambient curing. To achieve the early reaction and good strength at the initial

✉ Kanish Kapoor
kapoork@nitj.ac.in

Paramveer Singh
paramveers.ce.19@nitj.ac.in

[1] Department of Civil Engineering, Dr B R Ambedkar National Institute of Technology, Jalandhar 144011, India

stages of curing either heat curing or calcium (Ca) rich mineral is required in the GC [9]. The heat curing can accelerate the geopolymer reaction and help to achieve an early setting along with good strength of GC [10]. However, heat curing cannot be done at site conditions. Contrary to this, various Ca-rich minerals such as GGBS and PC are used as a partial replacement for geopolymer binder to provide the extra nucleation sites along with polymeric chain to achieve early setting time and good strength at the initial stage of curing [11]. Nagajothi and Elavenil [12] conclude that the addition of GGBS produces Ca hydrates along with a geopolymer matrix to improve the overall properties of GC. Nath and Sarker [13] also revealed that the addition of PC provides the Ca-rich hydrate gel which as a result enhances the properties of GC. According to other researchers, GGBS and PC addition enhances the performance of GC [14, 15].

The waste generated from construction and demolition is also a main concern due to the increase in renovation, upgradation and development of new infrastructure. The waste produced from construction and demolition becomes a challenge for society as it is increasing every year. The extent of concrete waste produced from construction and demolition is approximately 25–30%, and this waste can be further used as recycled aggregates in construction works [16]. The recycled aggregates are further categorized as coarse (> 4.75 mm) and fine (< 4.75 mm) aggregates. The 40–50% part of recycled aggregates consists of fine particles (< 4.75 mm) [17]. These fine particles of recycled aggregates contain 25–30% of anhydrate particles of cement along with hydrated cement particles, ettringites, Ca hydrates and anhydrate cement particles [18–20]. The anhydrate particles of cement present in recycled aggregates can help in providing additional hydration production along with conventional hydration in the production of concrete and mortar [21]. In a few studies, fine particles of recycled aggregates used in a grinded form called recycled mortar powder (RMP) in geopolymer mortar/concrete provide the extra nucleation sites with geopolymer polymeric chain due to the presence of anhydrate Ca compounds in RMP [22]. Ahmari et al. [23] utilized RMP as a partial replacement of FA and concluded that 50% content of RMP can be used to enhance the performance of the geopolymer mortar. Sharma et al. [24] used RMP as a partial replacement for binders and concluded that the inclusion of RMP helps to provide early activation to the geopolymer mortar and enhance their properties.

The literature studies revealed that GGBS or PC was extensively used in the GC to gain early strength and catalyze the geopolymerization in GC. However, very minimal information is available related to the utilization of RMP to provide early activation in the GC or mortar. Further, no study is available to access the durability properties of GC incorporating RMP. The key objective of the present study was to evaluate the durability properties of GC such as capillary suction test (CST), initial surface absorption test (ISAT) and acid attack at 28, 56 and 120 days of ambient curing. Furthermore, the ultrasonic pulse velocity (UPV) test and electrical Resistivity test have been performed to observe the quality and risk of corrosion to the GC, respectively. The compressive strength of GC was also evaluated in terms of strength property at 7, 28, 56 and 120 days. The RMP gives bi-fold benefits i.e., provides anhydrate Ca compounds for early activation of GC and contributes to the sustainability by being consumed as a concrete waste.

Materials used in experimental work

In this experimental work, the Class-F FA IS 3812:2013 [25] was used as a primary binder along with alkaline solutions and aggregates. The FA was collected from a nearby thermal plant located at Rajpura, Punjab, India. Further, RMP was partially substituted with FA in the GC mixes. The RMP was prepared using old concrete specimens available in the Concrete Technology Laboratory of the Authors Institute. The old concrete was available in the form of tested cubes, cylinders and prisms with compressive strength in the range of 20–35 MPa with a maximum age of approximately 2 years. The old concrete specimens were made of PC, natural coarse and fine aggregates and their physical and chemical properties are given in Table 1. In the first step, a jaw crusher was used to crush the old concrete specimens into small pieces and further sieved through a 2.36 mm sieve to produce RMP. The sieved fine particles of old concrete were kept in the oven at a temperature of 100 ± 5 ºC for 24 h to remove the moisture, if any. In the next step, the oven-dried fine particles of old concrete were ball milled for 8 h at 50 rpm to get particle size less than 75 microns to get the final product as

Table 1 Approximate physical properties and chemical composition of PC, coarse and fine aggregates of old concrete

Properties	PC	Coarse aggregates	Fine aggregates
Specific gravity	3.15	2.62	2.48
Water absorption	–	0.50%	1.5%
SiO_2	20%	60%	93%
Al_2O_3	6%	1%	2%
Fe_2O_3	5%	1%	0.50%
CaO	60%	15%	1%
MgO	3%	11%	0.2%
Na_2O	1%	0.50%	0.4%
K_2O	1%	1.63%	1%
SO_3	1%	0.1%	0.05%
P_2O_5	0.01%	0.02%	0.01%
TiO_2	0.50%	0.01%	0.01%
Loss of ignition	1.5%	10%	0.1%

RMP. The physical and chemical properties of FA and RMP are given in Table 2. Further, the particle distribution curve of FA and RMP is given in Fig. 1. The morphology of FA and RMP has been accessed using scanning electron microscopy (SEM), Fig. 2a, b. Figure 2a shows the SEM image of FA particles having a spherical shape with a smooth surface and on the other hand, the RMP particle has an irregular shape and rough surface, Fig. 2b.

The combination of SH and SS as an alkali solution was used in the experimental work. The SH solution was prepared using 98% pure pellets and mixed with appropriate water content to get a 12-molar solution. Further, SS was used in a liquid state and combined with SH in the ratio of 2.2:1 to form an alkaline solution. The properties of SH and SS are given in Table 3. Furthermore, coarse and fine aggregates were used in the experimental work confirming to IS 383:2016 [24]. The coarse aggregates of a maximum size of 12.5 mm and less than 4.75 mm size of fine aggregates were used for the experimental study. The physical properties of both coarse and fine aggregates are given in Table 4.

Table 2 Physical and chemical properties of FA and RMP

Properties	FA	RMP
Fineness, cm^2/gm	4125	3500
Specific gravity	2.1	2.5
SiO_2	56.50%	60.0%
Al_2O_3	22.50%	11.0%
Fe_2O_3	11.0%	4.0%
CaO	3.20%	15.0%
MgO	1.25%	2.5%
Na_2O	0.15%	1.85%
K_2O	2.2%	2.50%
SO_3	0.25%	1.25%
P_2O_5	0.6%	0.15%
TiO_2	2.2%	0.65%
Loss of ignition	1.20%	1.80%

Mix proportion and preparation of GC

The GC was prepared using FA (Class-F) as a main binder along with alkaline solution and aggregates. The RMP was partially substituted with FA in the range of 0%, 10%, 20%, 30%, 40% and 50% using an equivalent volumetric approach. The mix design method and factors used for mix design for the control mix were obtained from the literature [26]. The mix design factors such as alkali to binder ratio, SH molarity, SS to SH ratio and water to solid ratio were fixed to 0.47, 12 molarity, 2.2 and 0.35, respectively for all GC mixes. The GC mix proportions and notations made with varying content of RMP are given in Table 5. The GC was prepared by two-stage mixing. In the first stage, binders and aggregates were mixed thoroughly for 5–10 min in a drum-rotating mixer. In the second stage, the combination of SH and SS was poured and further mixed for 8–10 min to get a uniform geopolymer paste. The freshly prepared GC was then poured into molds and wrapped with a poly wrap to avoid moisture loss. The ambient curing was done to specimens until the age of testing at room temperature.

Testing procedures

The compressive strength of the GC specimens made with varying content of RMP was measured in accordance with IS 516:1959 [27]. The 100 mm cubes were used and an average of three specimens were taken as final compressive strength at a curing period of 7, 28, 56, and 120 days. The CST was conducted in conformation to the ASTM C1585-04 [28] on the specimen size of 100 mm × 50 mm (diameter × depth). The disc specimens were placed in the oven to achieve

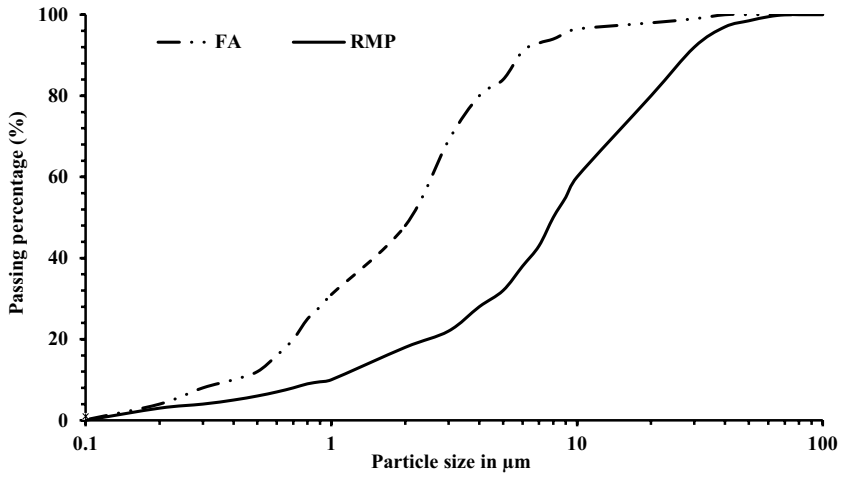

Fig. 1 Particle distribution curve of FA and RMP used in the experimental work

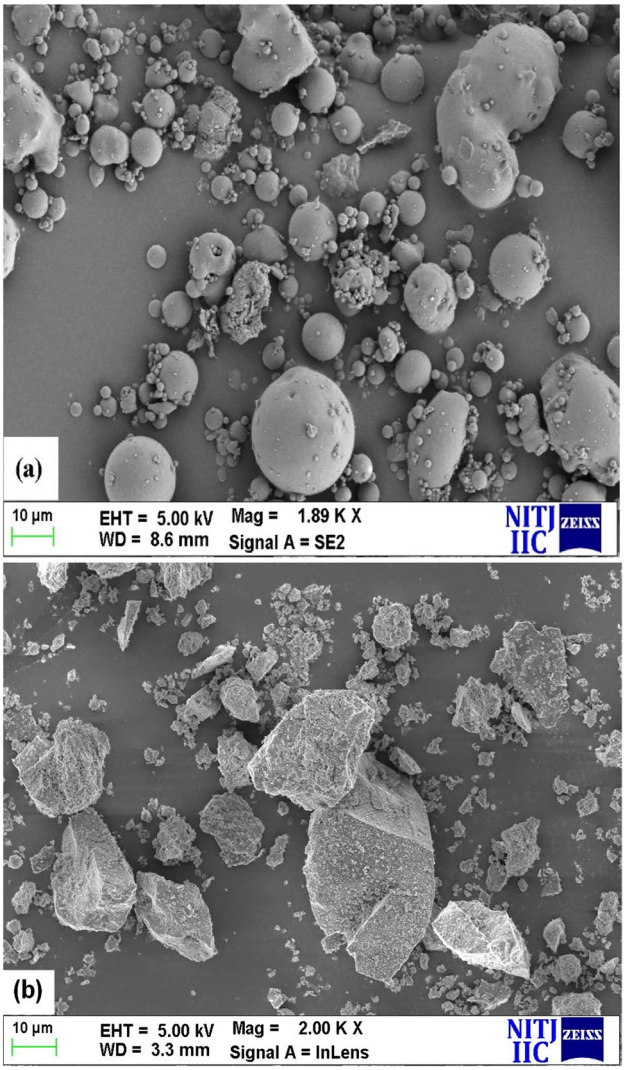

Fig. 2 SEM images of **a** FA and **b** RMP

Table 3 Properties of alkaline activators

Property	SH	SS
Molecular formula	NaOH	Na_2SiO_3
pH	13–14	13–14
Specific gravity	1.32	1.53
Na_2O content (%)	–	14.7
SiO_2 content (%)	–	29.4
H_2O content (%)	–	55.9

constant mass and further kept in a desiccator to bring these to ambient temperature. The sides of the specimens were sealed using wax and then packed loosely with a plastic sheet. The capillary suction values were recorded in terms of initial rate of absorption (IRA) up to 6 h at various intervals as given in the standards. The ISAT was conducted on the

Table 4 Physical properties of coarse and fine aggregates used in experimental work

Physical properties	Coarse aggregates	Fine aggregates
Specific gravity	2.65	2.53
Aggregate crushing value	15.50%	–
Aggregate impact value	15.35%	–
Water absorption	0.50%	1.55%

150 mm cubes as per BS 1881–208:1996 [29]. The specimens were kept in an oven to achieve constant mass and then kept in a desiccator to bring these to ambient temperature. The initial surface absorption was recorded in terms of ISA-10 (ISA at 10 min) as per standard. The acid attack of GC was conducted using a 5% concentration of sulphuric acid (H_2SO_4) at an exposure period of 28, 56, and 120 days as per ASTM C267 [30]. The specimens were first weighed before being exposed to the sulphuric acid. After being placed in acidic solutions at different intervals, the specimens were removed, weighed and dried for another 24 h at 100 ± 10 °C. Finally, the specimens were weighed to evaluate the weight loss due to exposure to the acid. During the soaking period, the acid water was replaced at 7-day intervals. The UPV test was done on 100 mm cube specimens in accordance with IS 13311:1992 [31] 56 and 120 days of recorded in meters/second as per standard. The electric resistivity of GC was examined on cylinders of 100 mm × 200 mm (diameter × depth) in accordance with ACI 222R-01 [32]. The surface of the specimens was saturated with water before performing the test so that voltage could be conducted through concrete to observe the readings of electrical resistivity values. The electrical resistivity was recorded in the kilo-ohms cm. The above-discussed test was performed at curing ages of 28, 56 and 120 days.

The microstructure analysis of GC mixes was done after 28 days of ambient curing. The SIGMA 500VP field emission scanning electron microscope (FESEM) machine was used for microscopy of GC mixes with varying content of RMP. Further, Fourier transform infrared (FTIR) spectroscopy was done on GC specimens to evaluate the geoplymerization and formation of various compounds with the addition of RMP.

Results and discussion

Effect of RMP on compressive strength of GC

The compressive strength results of GC mixes with varying replacements of RMP are shown in Fig. 3. The compressive strength is enhanced with the increasing content of RMP. For a mix with 10% RMP i.e., for GCR10, the

Table 5 Mix proportioning of GC mixes made with RMP in kg/m^3

Mix notation	Mix description	FA	RMP	SH	SS	Coarse aggregates	Fine aggregates	Additional water
GCR0	100% FA + 0% RMP (Control mix)	450	0	66	145	912	695	21.74
GCR10	90% FA + 10% RMP	405	54	66	145	912	695	21.74
GCR20	80% FA + 20% RMP	360	107	66	145	912	695	21.74
GCR30	70% FA + 30% RMP	315	161	66	145	912	695	21.74
GCR40	60% FA + 40% RMP	270	214	66	145	912	695	21.74
GCR50	50% FA + 50% RMP	225	268	66	145	912	695	21.74

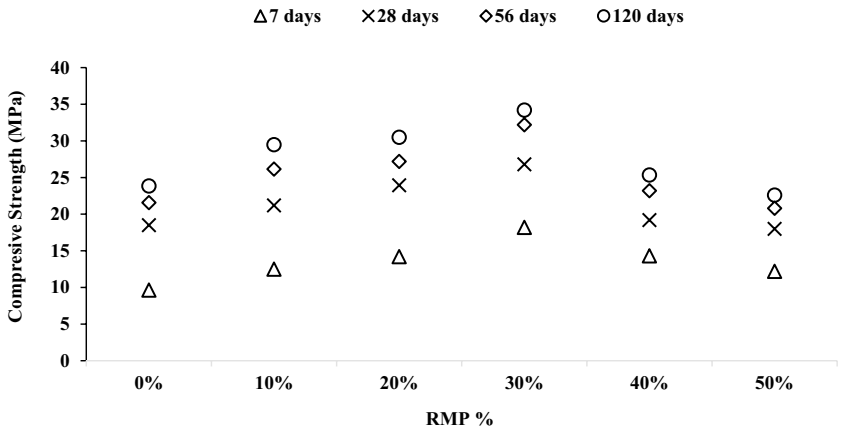

Fig. 3 Compressive strength of GC mixes with varying content of RMP

rise in compressive strength was 30% at the initial stage of 7 days relative to the GCR0. At a later stage of ambient curing, compressive strength enhanced in the range of 15–21% between 28 and 120 days compared to GCR0. Similarly, for mix GCR20, the compressive strength improved by 47% after 7 days and from 28 to 120 days, strength increased in the range of 26–30%. The Ca compound in the form of unreacted cement particles in RMP reacts with the silica and alumina content of binder (FA) to form additional calcium-alumino-silicate hydrate gel in the geopolymer matrix along with the geopolymer process, which tends to increase the compressive strength of GC. Further, with the substitution of 30% RMP with FA, the compressive strength increased very prominently at all ages of curing in comparison to all other GC mixes. For mix GCR30, the compressive strength increased by 89% and 45% at 7 and 28 days, respectively in contrast to the GCR0. In line with this, compressive strength enhanced by 49% and 44% at 56 and 120 days, respectively. The other researchers also claimed that the addition of Ca-rich compound improves the strength parameter of GC [33, 34].

Furthermore, with a 40% RMP (GCR40) mix, the compressive strength after 7 days was enhanced by 48% relative to GCR0. At a later stage of curing, i.e., after 120 days compressive strength increases marginally. Similarly, for GCR50, the compressive strength enhanced by 27% after 7 days and decreased marginally at later stages of curing in comparison to the GCR0. The results show that addition of RMP beyond 30%, the compressive strength declines in comparison to the GCR30 but is still at par with the compressive strength of the GCR0. The Ca present in the RMP contains, i.e. anhydrate particles and calcium-hydrated products. However, an increase in the content of RMP in GC increases the composition of both Ca anhydrate and hydrated particles. The anhydrate Ca particles react with the silica content of the alkaline solution and binder of GC to form additional nucleation sites. Moreover, the addition of a higher content of RMP also increases the content of Ca compounds which hinders the production of the calcium-alumina-silicate-hydrate gel after complete consumption of the silica content of the alkaline solution. In addition to this, the replacement of FA with RMP at a higher level decreases the composition of both unreacted silica and alumina which also hinders the geopolymer reaction which tends to decrease the compressive strength of the compressive strength of GC [22]. The overall findings show that, compared to later curing stages, the compressive strength enhanced significantly at 7 days of curing with the substitution of RMP. Based on the compressive strength results, 30% of RMP can be utilized with FA in the production of GC.

Effect of RMP on initial surface absorption of GC

The observed values of initial surface absorption of GC made with varying content of RMP are shown in Fig. 4. For mix GCR10, i.e., with the addition of 10% RMP, the ISA-10 values decreased in the range of 17 to 20% in between 28 and 120 days relative to the GCR0. Similarly, with the further inclusion of RMP up to 30% in GC, water ingress in GC through their surface decreases. For example, for mix GCR20, the ISA-10 declined in the range of 28%, 24% and 32% at 28, 56 and 120 days, respectively in contrast to the 0% RMP GC mix. Similarly, for mix GCR30, the surface absorption declines in the same trend as GCR20. The decrease is 29% and 27% after 28 and 56 days, respectively and it reached 38% after 120 days relative to the GCR0. The significant decrease in the ISA-10 values is due to the densified microstructure provided by the extra nucleation sites provided by RMP along with the geopolymer matrix. The presence of RMP along with the FA increases the pore-blocking effect which tends to resist the water penetration in the GC through the surface of concrete. In a previous study on geopolymer mortar, it was stated that substitution of RMP up to 30% decreases water absorption [24].

Further with the substitution of FA with RMP beyond 30%, the ISA-10 values start increasing for the GC. For example, for mix GCR40 (40% RMP), the ISA-10 values rise near about 10% at all stages of curing relative to the GCR0. Likewise, for mix GCR50, the ISA-10 values increase significantly at 28 days by 50% and there is a 35% and 25% increase in ISA-10 values after 56 and 120 days. The rise in ISA-10 values with the increase in RMP is due to an increase in silica content along with Ca compounds in the geopolymer matrix because, after the initial reaction of RMP and FA with an alkaline solution, the excessive silica gets unreacted and retards the geopolymeric reaction. Moreover, hydrated particles of RMP also tend to absorb more water which also tends to increase the water absorption of GC. The observed results of ISAT values of GC mixes recommended that the addition of RMP up to 30% helps to resist the surface absorption of water of GC significantly.

Effect of RMP on capillary suction of GC

The observed results of capillary suction values with the inclusion of RMP are shown in Fig. 5. For mix with the addition of 10% RMP, the IRA values decreased in the range of 35 to 51% between 28 and 120 days compared to the GCR0. Similarly, for mix GCR20, there was a significant drop in IRA values in the range of 56–77% between 28 and 120 days relative to the GCR0. The additional development of hydration gel due to the presence of RMP filled the micropores and resisted the water from penetrating the GC which in turn reduced the capillary suction of GC. Moreover, RMP provides pore refinement in the geopolymer matrix which as a result decreases the water penetration through capillary action in GC. Similarly, for mix GCR30 i.e., with the addition of 30% RMP, the IRA values decrease in the same trend in the range of 60 to 78% between 28 and 120 days in comparison to the mix made with 100% FA (GCR0).

Further, with the replacement of 40% FA with RMP i.e., GCR40 GC mix, the IRA values increase with respect to GCR30 at all stages of curing. On the other hand, the capillary suction is still lower than the control mix for the GCR40 mix. In comparison to the GCR0, the IRA values dropped in the range of 25–33% between 28 and 120 days. However, in comparison to the GCR30, the IRA values increase in the range of 30–49% up to 120 days. For mix GCR50, the IRA values increased marginally at all stages of curing in contrast to the 0% RMP mix. It shows that increasing the content of RMP tends to increase the permeability of GC through capillary action. The substitution of RMP in higher amounts in GC is left unreacted partially and loosens the microstructure which may increase the IRA values of GC.

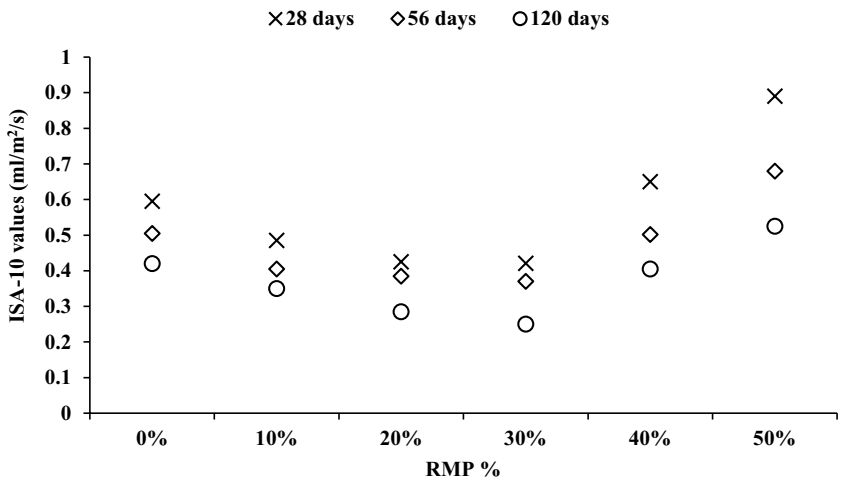

Fig. 4 ISA-10 of GC mixes with varying content of RMP

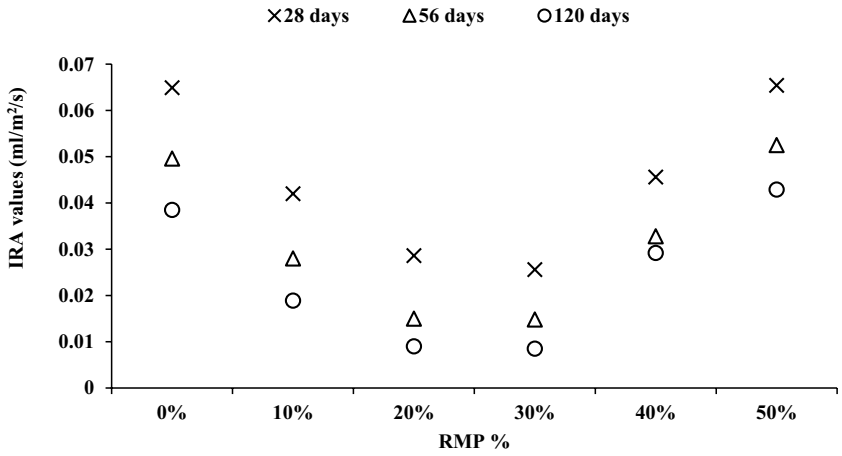

Fig. 5 IRA of GC mixes with varying content of RMP

As a result of capillary suction, it was observed that 40% RMP can be utilized in the GC.

Effect of RMP on acid exposure for GC

The percentage weight loss of GC mixes due to exposure to sulphuric acid is shown in Fig. 6. The weight loss of all GC mixes with the addition of RMP is negligible. For mix GCR0, the maximum weight loss was 5% up to 120 days of exposure to the sulphuric acid. The calcium sulphates and calcium alumino sulphates generally cause the deterioration of the concrete which is generated through an acid reaction with Ca present in the binder. However, FA (Class-F) used in the present study has low Ca content which restricts the production of the sulphate products, therefore, it shows a negligible effect on FA-based GC. For mix GCR10 (10% RMP), the decrease in weight is negligible up to 56 days of exposure and weight loss is 4% at 120 days of exposure to the sulphuric acid. Similarly, for the GCR20 and GCR30 GC mix, there is no significant effect during exposure to the sulphuric acid for up to 120 days. It shows that the addition of RMP has no reasonable effect on the acid exposure of the GC. Furthermore, with the addition of the 40% RMP, the weight loss of GC is less than 5% at 28 and 56 days of exposure period and it rises to 8% at 120 days of sulphuric acid exposure. Similarly, for mix GCR50, the maximum weight loss was 10% at 120 days of exposure period. The insignificant weight loss after 120 days of sulphuric acid exposure was due to the reaction of sulphates with alumino-silicate structure and their dealumination which tends to de-bond the paste and aggregates from concrete matrix [35]. The overall result of the acid attack shows that substitution of RMP up to 50% does not deteriorate the GC significantly even after 120 days of acid exposure.

Effect of RMP on UPV of GC

The observed values of UPV of GC mixes with the inclusion of RMP are given in Fig. 7**.** The substitution of RMP in GC has an insignificant effect on the UPV values. For mix GCR10, the UPV values increased marginally by 3% and 4% after 28 and 56 days, respectively and reached 8%

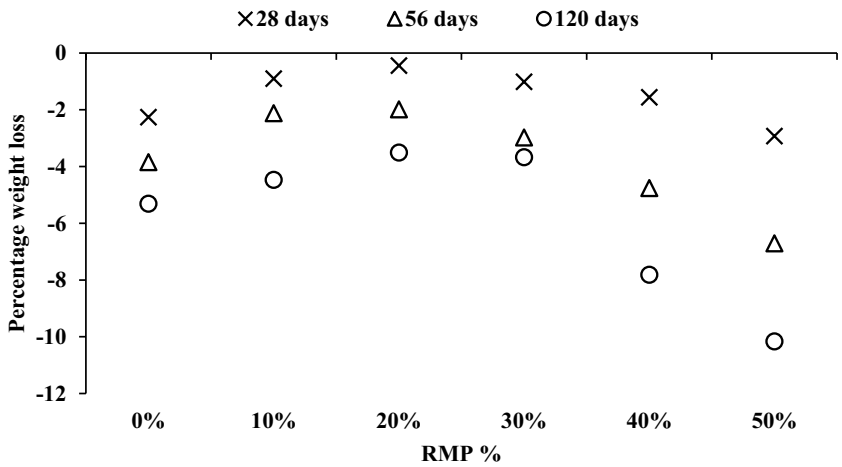

Fig. 6 Percentage weight loss of GC mixes with varying content of RMP

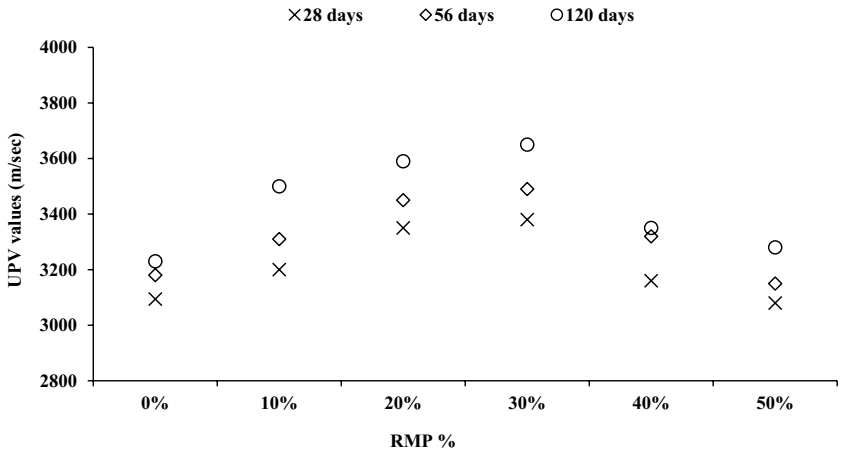

Fig. 7 UPV of GC mixes with varying content of RMP

after 120 days in comparison to GCR0. For mix GCR20, the increase in UPV values is 8% at both 28 and 56 days. At 120 days, the UPV values increased by 11% in comparison to the GCR0. Similarly, for the GC mix with the addition of 30% RMP, the UPV values enhanced by 9% at both 28 and 56 days whereas it reached 13% after 120 days. The production of Ca hydrates in the geopolymer matrix due to the presence of RMP makes the microstructure of the concrete denser, which increases the sound wave velocity and increases the UPV values of GC. The substitution of RMP in conventional cement concrete also gives positive results of UPV [36, 37]. The UPV values increase in the same trend as compressive strength with the inclusion of RMP in GC. For mix GCR40 and GCR50, the UPV values decreased marginally relative to the control mix GCR30 but still at equivalence with the GCR0. The slight reduction in the UPV values was due to the high porosity of RMP which may restrict the path of sound waves to travel uniformly. The UPV values of GCR10, GCR20 and GCR30 come in the good category as per standard limits after 120 days of curing and the rest GC mixes come under satisfactory conditions.

Effect of RMP on the electrical resistivity of GC

The electrical resistivity values of GC made with RMP are presented in Fig. 8. The results shown in the figure revealed that the change in electric resistivity values was insignificant for GC made with RMP. For mix GCR10, the electrical resistivity values increased marginally by 6% at all ages of curing relative to the GCR0. Further with the addition of 20% RMP, i.e., GCR20 the electrical resistivity values increased in the range of 14 to 16% in between 28 and 120 days relative to the GCR0. The inclusion of RMP densifies the microstructure of GC by reducing the interconnected pores as discussed in the preceding sections which as a result tends to restrict the ingress of chlorides and there is a low risk of corrosion in concrete [38]. Similarly, for mix GCR30, the electric resistivity values increased less than 10% at all ages of curing relative to the GCR0. However, in comparison to the GCR20, the electrical resistivity values start decreasing. Furthermore, with the inclusion of RMP beyond 30%, the electrical resistivity values decline in contrast to the 0% RMP mix. For the GCR40 mix, the electrical

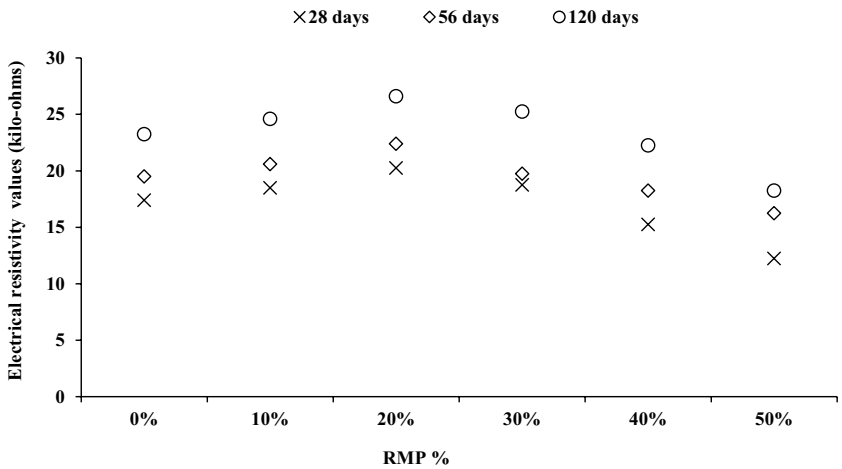

Fig. 8 Electrical resistivity of GC mixes with varying content of RMP

resistivity values decreased by 12%, 6% and 4% after 28, 56 and 120 days, respectively relative to the GCR0. Similarly, for the GC mix with 50% RMP, the electrical resistivity values decreased significantly in the range of 22 to 30% between 28 and 120 days of curing, respectively in contrast to the GCR0 mix. The higher content of RMP increases the pore volume in concrete which a result gives free movement of foreign particles in GC which a result tends to decrease the electrical resistivity of GC. The overall analysis shows that for all geopolymer mixes the electrical resistivity values are in low risk of corrosion range after 120 days of curing except GC mix with 50% RMP.

Microstructural analysis

SEM analysis of GC with varying content of RMP

The SEM analysis of GC mixes with 0%, 30% and 50% RMP are presented in Fig. 9a–c. The GC mix with 0% RMP (control mix), the alumina-silicate binder i.e., FA dissolute with OH^- ions to form a sialate bond called a geopolymer matrix as shown in Fig. 9a. The formation of the geopolymer matrix in concrete results gives a compressive strength of 18.5 MPa after 28 days. On the other hand, there are some macro- and micro-cracks present which may increase the water ingress in the GC. Ren et al. [22] observed that 0% RMP concrete has a denser microstructure than GC with RMP due to the presence of cracks. In opposition to this, with the addition of RMP i.e. for GCR30 (30% RMP) GC mix, the presence of Ca compound in RMP produced calcium alumina-silicate hydrate gel with geopolymer matrix as shown in Fig. 9b and densified the microstructure of GC which in result enhance the overall properties of GC. As discussed in the above section, the compressive strength of GCR30 increased prominently by 89% at 7 days and 45% at 28 days of ambient curing relative to the GCR0. Similarly, capillary suction and initial surface absorption of water decreases with the addition of 30% RMP. The literature study also claims that the addition of a Ca-rich compound generated hydration products along with geopolymerization which in turn made a dense microstructure of GC [39]. Similarly, with the addition of RMP beyond 30%, i.e., for 50% RMP GC mix, the Ca hydrate gel is produced gradually with the geopolymer matrix. However, the high content of RMP tends to decrease the packing density of GC due to their irregular surface and hydrated compounds. Figure 9c also shows some

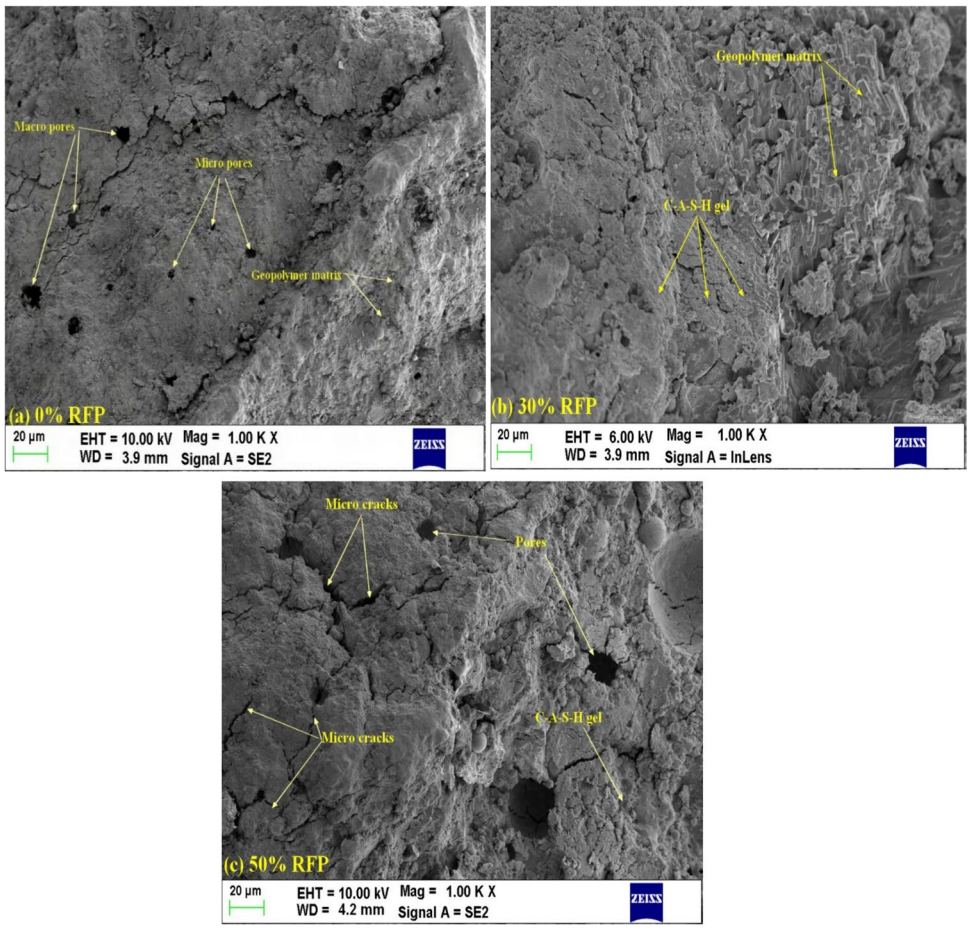

Fig. 9 SEM images of GC mixes **a** GCR0, **b** GCR30 and **c** GCR50

cracks and pores in the geopolymer matrix with the higher content of RMP which tends to deteriorate the strength and durability properties. Additionally, compared to other GC mixes, RMP's presence of hydrated particles increases water absorption and porosity, which in turn increases capillary suction and surface absorption of GC. The overall microscopic analysis illustrates that the substitution of RMP up to 30% with FA gives optimum results in terms of strength and durability properties and a further increase in RMP content mainly effect the durability properties of GC due to the heterogeneous structure of RMP and hydrated compounds present in the RMP.

FTIR analysis of GC made with varying content of RMP

The infrared spectra analysis of GC mix with 0%, 30% and 50% of RMP are shown in Fig. 10a–c. The GC mix with 0% RMP, i.e., GCR0, shows a peak at 450 cm^{-1} i.e., due to irregular Si–O (Al) stretching and related to that sharp peak was detected at 1000 cm^{-1} due to planer tetrahedral Si–O bending, Fig. 10a. The spectra observed for the GCR0 GC mix are matched with a previous study [34]. Similarly, the medium peak observed near about 775 cm^{-1} shows Si–O vibrations due to the presence of initial Si in FA [40, 41]. The presence of Si–O (Al) vibrations at different peaks shows that the geopolymer matrix was generated through the geopolymerization of FA with alkali solutions to form the final product. The same has been observed through SEM images as discussed in the above sections. Further, for GC mix with 30% RMP i.e., GCR30, the peaks were observed near about 450 cm^{-1}, 775 cm^{-1} and 1000 cm^{-1} which shows the Si–O bonds of stretching and bending similar to GCR0 GC mix, Fig. 10b. In addition to this, other peaks were also observed at 1400 cm^{-1} and 3000 cm^{-1} in the spectra of the GCR30 GC mix. The weak and broad peak near bout 1400 cm^{-1} shows the new phase of alumina-silicate

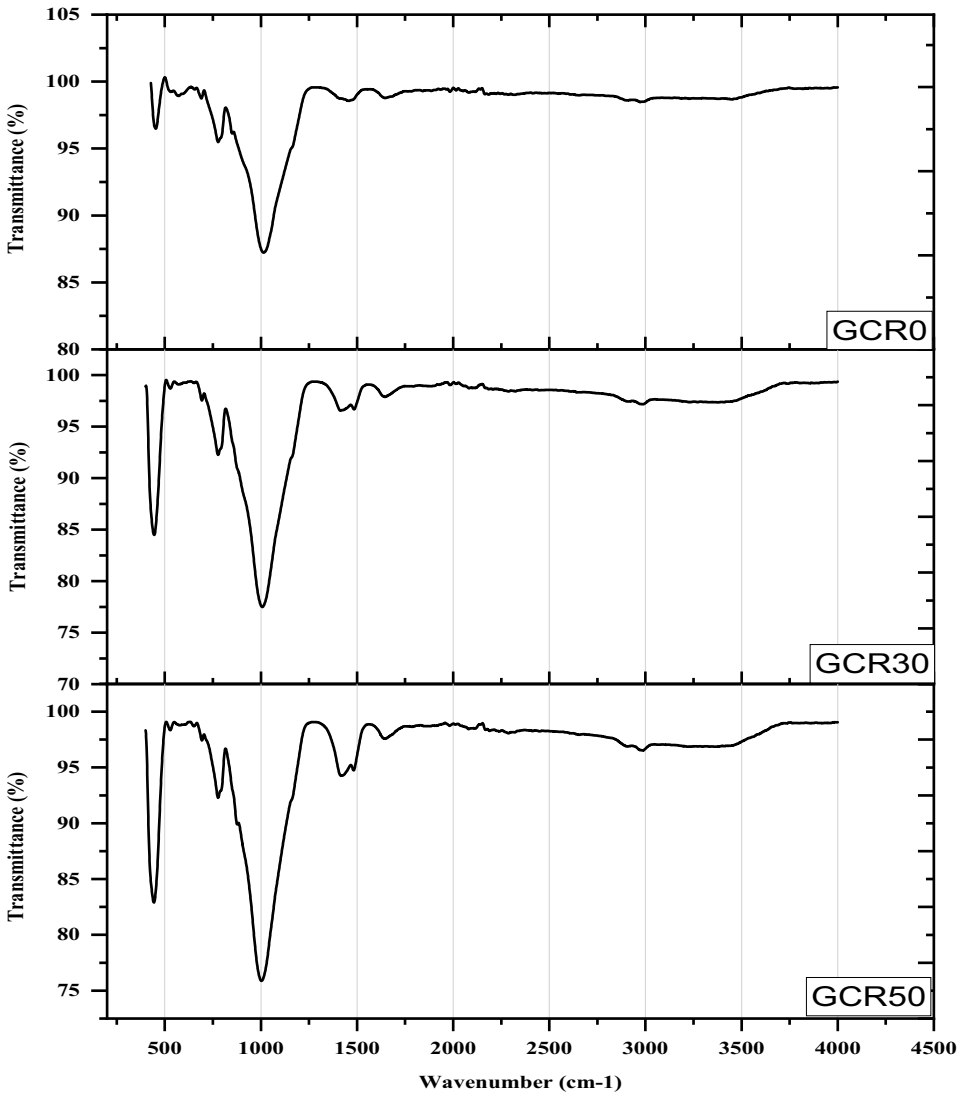

Fig. 10 FTIR analysis of GC mixes **a** GCR0, **b** GCR30 and **c** GCR50

of geopolymer reaction. The lower peak was observed due to the formation of C-A-S-H gel which is more crystalline than the geopolymer matrix [23, 42]. On the other hand, the weak and broad peak near about 3000 cm^{-1} shows the O–H stretching which also helps to produce hydration gel along with geopolymer matrix. The same has been discussed in SEM analysis that with the addition of RMP, the hydrates were formed along with the geopolymer matrix. Further, the addition of 50% RMP shows the same trend of spectra with marginal lower peaks in comparison to the GCR30 GC mix, Fig. 10c. The reduction in spectra was due to the addition of a higher content of Si and Ca which lowers the absorbance. The overall analysis shows that GC mixes with the addition of RMP show sharper peaks in comparison to the 0% RMP mix (GCR0) which revealed that GCR0 is amorphous than GCR30 and GCR50 GC mix.

Correlation of properties with varying content of RMP

The variation of compressive strength and durability properties with the varying content of RMP at 28 days of curing is shown in Fig. 11. The compressive strength starts increasing with the addition of RMP at 10%, 20% and 30% replacement with FA as shown in Fig. 11. It starts declining with the addition of RMP beyond 30%. On the other hand, the ISAT values and IRA values start decreasing significantly up to 30% addition of RMP and start increasing beyond 30% addition of RMP. The decrease in ISAT and IRA values shows a decrease in the permeability of concrete with the addition of RMP. It shows that the addition of RMP up to 30% helps to enhance the overall properties with the formation of extra hydration products along with the geopolymer matrix of GC as confirmed with microstructure analysis of GC with the addition of RMP. Further, UPV values also enhanced up to 30% addition of RMP. The electrical resistivity values are higher than the control mix up to 30% addition of RMP and start decreasing with further addition of RMP. The overall correlation of properties shows that a 30% addition of RMP is the optimum content in the GC which enhances the overall properties of GC.

Conclusions

GC's strength and durability were significantly improved with the addition of RMP. The use of RMP has two benefits: it enhances the overall characteristics of GC by providing nucleation sites with a geopolymer matrix, and it promotes sustainability by being used as concrete waste.

1. The GC mixes made with RMP show improved compressive strength than the 0% RMP mix. The compressive strength is enhanced significantly with the inclusion of RMP up to 30%, beyond the 30% addition of RMP and it starts decreasing with respect to the GCR30 mix but still higher than the GCR0 (control mix). Additionally, due to the presence of Ca compounds in RMP, the increase in compressive strength with the addition of RMP is prominent at 7 days compared to the later stages of curing.
2. The initial surface absorption of water in the GC mix gets reduced with the inclusion of RMP up to 30% and after that water surface absorption of GC increases with the increase in the content of RMP. The densified microstructure formation at 30% RMP shows water ingress gets restricted in the GC.
3. The water absorption in GC through capillary suction gets restricted up to 40% addition of RMP. The presence

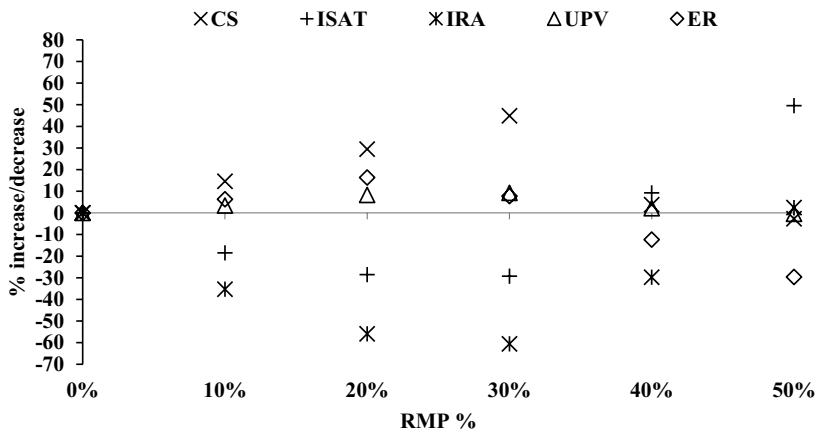

Fig. 11 Correlation of properties of GC with varying content of RMP

CS – Compressive strength, ER – Electrical resistivity

of Ca compound in RMP forms the additional gel along with geopolymer matrix which fills the micro pores in GC which tends to reduce to intake of water through capillary action.

4. There is no significant effect of sulfuric acid on GC with or without the presence of RMP. There is a maximum of 10% weight loss after 120 days of sulphuric acid exposure to GC with the inclusion of the 50% RMP.
5. The UPV values of GC mixes are enhanced with the substitution of RMP up to 30%. The GC mixes GCR10, GCR20 and GCR30 come under good category as per standard after 120 days of curing.
6. All GC mixes come under a low risk of corrosion corresponding to the electrical resistivity values except the GCR50 mix. The addition of RMP enhances the electrical resistivity of GC by forming additional nucleation sites along with a geopolymer matrix.
7. The microstructure analysis done in the form of SEM and FTIR of GC with the inclusion of RMP shows the presence of Ca compounds along with the geopolymer matrix. The SEM images show densified microstructure with the formation of calcium alumina-silicate hydrate gel with a 30% addition of RMP. The FTIR analysis concludes that the addition of RMP provides extra nucleation sites (O–H stretching) along with the Si–O bond in the GC.

Acknowledgements The financial assistance in the form of a fellowship to the first author from the Ministry of Education (MoE), Government of India, is appreciatively acknowledged. The authors also acknowledge the support of the staff of the Structures Testing Laboratory at Dr. B. R. Ambedkar National Institute of Technology, Jalandhar, India, during the experimentation work reported in the paper.

Funding This research was supported by Ministry of Education, India.

Data availability The authors confirm that the data supporting the findings of this study are available within the article.

Declarations

Conflict of interest The authors declare that they have no known competing financial interests or personal relationships that could have appeared to influence the work reported in this paper.

References

1. Huntzinger DN, Eatmon TD (2009) A life-cycle assessment of Portland cement manufacturing: comparing the traditional process with alternative technologies. J Clean Prod 17:668–675. https://doi.org/10.1016/J.JCLEPRO.2008.04.007
2. Colangelo F, Farina I, Travaglioni M et al (2021) Eco-efficient industrial waste recycling for the manufacturing of fibre reinforced innovative geopolymer mortars: Integrated waste management and green product development through LCA. J Clean Prod 312:127777. https://doi.org/10.1016/j.jclepro.2021.127777
3. Saxena R, Gupta T, Sharma RK, Siddique S (2022) Mechanical, durability and microstructural assessment of geopolymer concrete incorporating fine granite waste powder. J Mater Cycles Waste Manag 24:1842–1858. https://doi.org/10.1007/s10163-022-01439-0
4. Shobeiri V, Bennett B, Xie T, Visintin P (2021) A comprehensive assessment of the global warming potential of geopolymer concrete. J Clean Prod 297:126669. https://doi.org/10.1016/J.JCLEPRO.2021.126669
5. Yadav VK, Gacem A, Choudhary N et al (2022) Status of coal-based thermal power plants, coal fly ash production, utilization in India and their emerging applications. Miner 12:1503. https://doi.org/10.3390/MIN12121503
6. Cong P, Cheng Y (2021) Advances in geopolymer materials: a comprehensive review. J Traffic Transp Eng (English Ed) 8:283–314. https://doi.org/10.1016/J.JTTE.2021.03.004
7. Dindi A, Quang DV, Vega LF et al (2019) Applications of fly ash for CO_2 capture, utilization, and storage. J CO2 Util 29:82–102. https://doi.org/10.1016/J.JCOU.2018.11.011
8. Alhawat M, Ashour A, Yildirim G et al (2022) Properties of geopolymers sourced from construction and demolition waste: a review. J Build Eng 50:104104. https://doi.org/10.1016/J.JOBE.2022.104104
9. Hassan A, Arif M, Shayiq M (2019) Effect of curing condition on the mechanical properties of fly ash-based geopolymer concrete. SN Appl Sci 112(1):1–9. https://doi.org/10.1007/S42452-019-1774-8
10. Kong DLY, Sanjayan JG (2010) Effect of elevated temperatures on geopolymer paste, mortar and concrete. Cem Concr Res 40:334–339. https://doi.org/10.1016/J.CEMCONRES.2009.10.017
11. Tee KF, Mostofizadeh S (2021) A mini review on properties of portland cement concrete with geopolymer materials as partial or entire replacement. Infrastructures 6:26. https://doi.org/10.3390/INFRASTRUCTURES6020026
12. Nagajothi S, Elavenil S (2020) Effect of GGBS addition on reactivity and microstructure properties of ambient cured fly ash based geopolymer concrete. SILICON 13:507–516. https://doi.org/10.1007/s12633-020-00470-w
13. Nath P, Sarker PK (2015) Use of OPC to improve setting and early strength properties of low calcium fly ash geopolymer concrete cured at room temperature. Cem Concr Compos 55:205–214. https://doi.org/10.1016/j.cemconcomp.2014.08.008
14. Mallikarjuna Rao G, Gunneswara Rao TD (2018) A quantitative method of approach in designing the mix proportions of fly ash and GGBS-based geopolymer concrete. Aust J Civ Eng 16:53–63. https://doi.org/10.1080/14488353.2018.1450716
15. Farhan NA, Sheikh MN, Hadi MNS (2018) Experimental investigation on the effect of corrosion on the bond between reinforcing steel bars and fibre reinforced geopolymer concrete. Structures 14:251–261. https://doi.org/10.1016/j.istruc.2018.03.013
16. Zhu P, Hua M, Liu H et al (2020) Interfacial evaluation of geopolymer mortar prepared with recycled geopolymer fine aggregates. Constr Build Mater 259:119849. https://doi.org/10.1016/j.conbuildmat.2020.119849
17. Diliberto C, Lecomte A, Aissaoui C et al (2021) The incorporation of fine recycled concrete aggregates as a main constituent of cement. Mater Struct Constr. https://doi.org/10.1617/s11527-021-01796-6
18. Ashiquzzaman M, Hossen S (2013) Cementing property evaluation of recycled fine aggregate. Int Ref J Eng Sci 2:63–68
19. Bian Y, Li Z, Zhao J, Wang Y (2022) Synergistic enhancement effect of recycled fine powder (RFP) cement paste and carbonation on recycled aggregates performances and its mechanism. J Clean Prod 344:130848. https://doi.org/10.1016/J.JCLEPRO.2022.130848

20. Hai HZ, Dong HX, Yuan ZM et al (2022) A novel development of green UHPC containing waste concrete powder derived from construction and demolition waste. Powder Technol 398:117075. https://doi.org/10.1016/J.POWTEC.2021.117075
21. Kapoor K, Singh SP, Singh B (2020) Permeability of self-compacting concrete made with recycled concrete aggregates and Portland cement-fly ash-silica fume binder. J Sustain Cem Mater. https://doi.org/10.1080/21650373.2020.1809029
22. Ren P, Li B, Yu J-G, Ling T-C (2020) Utilization of recycled concrete fines and powders to produce alkali activated slag concrete blocks. J Clean Prod 267:122115. https://doi.org/10.1016/j.jclepro.2020.122115
23. Ahmari S, Ren X, Toufigh V, Zhang L (2012) Production of geopolymeric binder from blended waste concrete powder and fly ash. Constr Build Mater 35:718–729. https://doi.org/10.1016/j.conbuildmat.2012.04.044
24. Sharma A, Singh P, Kapoor K (2022) Utilization of recycled fine powder as an activator in fly ash based geopolymer mortar. Constr Build Mater 323:126581. https://doi.org/10.1016/J.CONBUILDMAT.2022.126581
25. IS 3812 (2013) Specifications for Pulverized fuel ash, Part-1: for use as pozzolana in cement, cement mortar and concrete. Bur Indian Stand New Delhi, India 1–12
26. Singh P, Kapoor K (2022) Development of mix design method based on statistical analysis of different factors for geopolymer concrete. Front Struct Civ Eng 16:1315–1335. https://doi.org/10.1007/s11709-022-0853-x
27. IS 516 (1959) Method of tests for strength of concrete. Bur Indian Stand New Delhi
28. ASTM C1585 (2004) Standard test method for measurement of rate of absorption of water by Hydraulic-Cement Concrete. Am Soc Test Mater
29. BS 1881–208 (1996) Recommendations for the determination of the initial surface absorption of concrete
30. ASTM C267 Standard test methods for chemical resistance of mortars, grouts, and monolithic surfacings and polymer concrete
31. IS 13311 (Part I) (1992) Non-destructive testing of concrete test methods (Ultrasonic pulse velocity)
32. ACI Committee 222 (2001) Protection of metals in concrete against corrosion. ACI 222R:1–41
33. Dombrowski K, Buchwald A, Weil M (2007) The influence of calcium content on the structure and thermal performance of fly ash based geopolymers. J Mater Sci 42:3033–3043. https://doi.org/10.1007/S10853-006-0532-7/FIGURES/14
34. Lecomte I, Henrist C, Liégeois M et al (2006) (Micro)-structural comparison between geopolymers, alkali-activated slag cement and Portland cement. J Eur Ceram Soc 26:3789–3797
35. Valencia-Saavedra WG, Mejía de Gutiérrez R, Puertas F (2020) Performance of FA-based geopolymer concretes exposed to acetic and sulfuric acids. Constr Build Mater 257:119503. https://doi.org/10.1016/J.CONBUILDMAT.2020.119503
36. Cantero B, Bravo M, de Brito J et al (2020) Mechanical behaviour of structural concrete with ground recycled concrete cement and mixed recycled aggregate. J Clean Prod. https://doi.org/10.1016/j.jclepro.2020.122913
37. Aldawsari S, Kampmann R, Harnisch J, Rohde C (2022) Setting time, microstructure, and durability properties of low calcium fly ash/slag geopolymer: a review. Materials (Basel) 15:1–25. https://doi.org/10.3390/ma15030876
38. Salahuddin H, Qureshi LA, Nawaz A, Raza SS (2020) Effect of recycled fine aggregates on performance of Reactive Powder Concrete. Constr Build Mater 243:118223. https://doi.org/10.1016/j.conbuildmat.2020.118223
39. Rashad AM, Sadek DM, Hassan HA (2016) An investigation on blast-furnace stag as fine aggregate in alkali-activated slag mortars subjected to elevated temperatures. J Clean Prod 112:1086–1096
40. Ismail I, Bernal SA, Provis JL et al (2014) Modification of phase evolution in alkali-activated blast furnace slag by the incorporation of fly ash. Cem Concr Compos 45:125–135. https://doi.org/10.1016/J.CEMCONCOMP.2013.09.006
41. Hajimohammadi A, Provis JL, van Deventer JSJ (2011) Time-resolved and spatially-resolved infrared spectroscopic observation of seeded nucleation controlling geopolymer gel formation. J Colloid Interface Sci 357:384–392. https://doi.org/10.1016/J.JCIS.2011.02.045
42. Yunsheng Z, Wei S, Qianli C, Lin C (2007) Synthesis and heavy metal immobilization behaviors of slag based geopolymer. J Hazard Mater 143:206–213. https://doi.org/10.1016/J.JHAZMAT.2006.09.033